

Structure and Reactivity of the Cationic Nickel Compound $[(\eta^3:\eta^1\text{-Ind}(\text{CH}_2)_2\text{NMe}_2)\text{Ni}(\text{PPh}_3)][\text{BPh}_4]$

Laurent F. Groux and Davit Zargarian*

Département de chimie, Université de Montréal, Montréal, Québec, Canada H3C 3J7

Received March 13, 2001

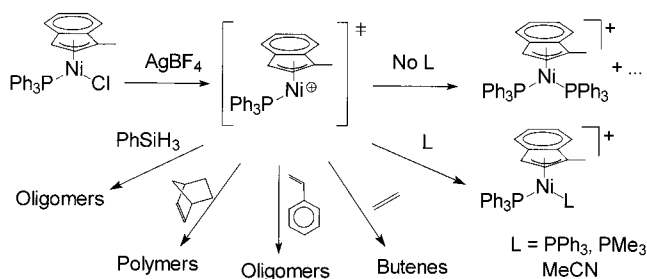
The solid-state structure of the first nickel compound containing a chelating amino-indenyl ligand, $[(\eta^3:\eta^1\text{-Ind}(\text{CH}_2)_2\text{NMe}_2)\text{Ni}(\text{PPh}_3)][\text{BPh}_4]$ (**2**), has been resolved and confirms the chelation of the amine tether to the nickel center. Complex **2** acts as a precatalyst for the oligomerization of norbornene, the dimerization of phenylsilane, and the polymerization of styrene. The results of these catalytic reactions are qualitatively different from those catalyzed by the cationic species generated in situ from the precursor complex $(\eta^3:\eta^0\text{-Ind}(\text{CH}_2)_2\text{NMe}_2)\text{Ni}(\text{PPh}_3)\text{Cl}$ (**1**). Phosphines displace the amine tether in **2** to give the bis(phosphine) cations $[(\eta^3:\eta^0\text{-Ind}(\text{CH}_2)_2\text{NMe}_2)\text{Ni}(\text{Ph}_2\text{PCH}_2\text{CH}_2\text{PPh}_2)]^+$ (**3**) and $[(\eta^3:\eta^0\text{-Ind}(\text{CH}_2)_2\text{NMe}_2)\text{Ni}(\text{PPh}_3)(\text{PR}_3)]^+$ (**4**, R = Ph; **5**, R = Me), whereas LiI reacts to form the neutral compound $[(\eta^3:\eta^0\text{-Ind}(\text{CH}_2)_2\text{NMe}_2)\text{Ni}(\text{PPh}_3)\text{I}]\cdot\text{LiBPh}_4$ (**7**). The displacement of the amine tether by pyridine and its methyl-substituted derivatives leads to an equilibrium between **2** and $[(\eta^3:\eta^0\text{-Ind}(\text{CH}_2)_2\text{NMe}_2)\text{Ni}(\text{PPh}_3)\text{L}]^+$ (**6**) with K_{eq} values of 9 (**6a**, L = pyridine), 2.0 (**6b**, L = 2-picoline), 23 (**6c**, L = 3-picoline), 33 (**6d**, L = 4-picoline), and 16 (**6e**, L = 3,5-lutidine).

Introduction

During the course of our investigations¹ into the chemistry of the complexes $(\text{Ind})(\text{PPh}_3)\text{Ni}-\text{X}$ (Ind = indenyl and its substituted derivatives; X = halide, alkyl, alkynyl, imidate, thiolate, etc.), it was found that the in situ generated cationic species $[(\text{Ind})(\text{PPh}_3)\text{Ni}]^+$ can catalyze a number of reactions, including the dimerization of ethylene to butenes,^{1a,e} the dehydrogenative oligomerization of PhSiH_3 to $(\text{PhSiH})_n$,^{1d} the oligomerization of styrene, the polymerization of norbornene, and the copolymerization of styrene and norbornene. In situ generated $[(\text{Ind})(\text{PPh}_3)\text{Ni}]^+$ also reacts with phosphines or donor solvents such as MeCN to form the adducts $[(\text{Ind})(\text{PPh}_3)\text{NiL}]^+$; indeed, the electrophilicity of the “naked” cation is such that in the absence of added ligand and donor solvents it undergoes a redistribution reaction to form $[(\text{Ind})\text{Ni}(\text{PPh}_3)_2]^+$, which is catalytically inert (Scheme 1). The presence of this deactivation pathway has hindered further investigations into the structure and reactivities of these highly electrophilic cations.

In an effort to circumvent this deactivation of the unstable cations $[(\text{Ind})(\text{PR}_3)\text{Ni}]^+$, we set out to prepare analogous complexes bearing hemilabile coordinating moieties² which might stabilize the cationic intermediates sufficiently to allow isolation and characterization

Scheme 1. Reactivity of $[(1\text{-MeInd})\text{Ni}(\text{PPh}_3)]^+$



while maintaining catalytic activity. Aminoindenyl ligands were chosen for this purpose because it was anticipated that (a) the proximity of the amine-functionalized tether to the nickel center would facilitate N→Ni coordination and prevent the formation of the inert bis(phosphine) species and (b) the lower affinity of the amine moiety, relative to phosphines, for coordination to nickel³ would not shut down the catalytic activity. In an earlier report,⁴ we described the preparation and complete characterization of the precursor complex $(\eta^3:\eta^0\text{-Ind}(\text{CH}_2)_2\text{NMe}_2)(\text{PPh}_3)\text{Ni}-\text{Cl}$ (**1**) and presented spectroscopic evidence for the formation of the

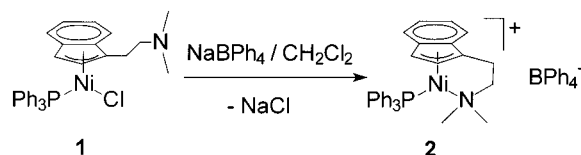
(1) (a) Dubois, M.-A.; Wang, R.; Zargarian, D.; Tian, J.; Vollmerhaus, R.; Li, Z.; Collins, S. *Organometallics* **2001**, *20*, 663. (b) Wang, R.; Bélanger-Gariépy, F.; Zargarian, D. *Organometallics* **1999**, *18*, 5548. (c) Dubuc, I.; Dubois, M.-A.; Bélanger-Gariépy, F.; Zargarian, D. *Organometallics* **1999**, *18*, 30. (d) Fontaine, F.-G.; Kadkhodazadeh, T.; Zargarian, D. *J. Chem. Soc., Chem. Commun.* **1998**, 1253. (e) Vollmerhaus, R.; Bélanger-Gariépy, F.; Zargarian, D. *Organometallics* **1997**, *16*, 4762. (f) Huber, T. A.; Bayraktarian, M.; Dion, S.; Dubuc, I.; Bélanger-Gariépy, F.; Zargarian, D. *Organometallics* **1997**, *16*, 5811. (g) Bayraktarian, M.; Davis, M. J.; Reber, C.; Zargarian, D. *Can. J. Chem.* **1996**, *74*, 2194. (h) Huber, T. A.; Bélanger-Gariépy, F.; Zargarian, D. *Organometallics* **1995**, *14*, 4997.

(2) Recent reviews on side-chain-functionalized cyclopentadienyl compounds: (a) Jutzi, P.; Redeker, T. *Eur. J. Inorg. Chem.* **1998**, 663. (b) Müller, C.; Vos, D.; Jutzi, P. *J. Organomet. Chem.* **2000**, *600*, 127.

(3) The generally stronger binding of phosphines vs amines to low-valent late transition metals is well-documented: (a) Collman, J. P.; Hegedus, L. S.; Norton, J. R.; Finke, R. G. *Principles and Applications of Organotransition Metal Chemistry*; University Science Books: Mill Valley, CA, 1987; p 241, and references therein. (b) Li, M. P.; Drago, R. S.; Pribula, A. J. *J. Am. Chem. Soc.* **1977**, *99*, 6900. (c) de Graaf, W.; Boersma, J.; Smeets, W. J. J.; Spek, A. L.; van Koten, G. *Organometallics* **1989**, *8*, 2907. (d) Wang, L.; Wang, C.; Bau, R.; Flood, T. C. *Organometallics* **1996**, *15*, 491. (e) Widenhoefer, R. A.; Buchwald, S. L. *Organometallics* **1996**, *15*, 2755. (f) Widenhoefer, R. A.; Buchwald, S. L. *Organometallics* **1996**, *15*, 3534. (g) Pfeiffer, J.; Kickelbick, G.; Schubert, U. *Organometallics* **2000**, *19*, 62.

(4) Groux, L. F.; Bélanger-Gariépy, F.; Zargarian, D.; Vollmerhaus, R. *Organometallics* **2000**, *19*, 1507.

Scheme 2. Preparation of
 $[(\eta^3:\eta^1\text{-Ind}(\text{CH}_2)_2\text{NMe}_2)\text{Ni}(\text{PPh}_3)][\text{BPh}_4]$



cationic complex $[(\eta^3:\eta^1\text{-Ind}(\text{CH}_2)_2\text{NMe}_2)\text{Ni}(\text{PPh}_3)][\text{BPh}_4]$ (**2**). The present paper reports the structural characterization of **2** and describes the ligand substitution reactions and catalysis arising from the displacement of the amine tether by various ligands.

Results and Discussion

Complex **2** can be prepared in ca. 60% yield by abstracting Cl^- from **1** in CH_2Cl_2 (Scheme 2).⁴ The $^{31}\text{P}\{\text{H}\}$ NMR spectrum of the product showed that the signal for the precursor (ca. 31 ppm) was replaced by a new singlet resonance (ca. 29 ppm). The absence of an AB resonance which is characteristic of the inequivalent P nuclei in the bis(phosphine) cations $[(1\text{-R-Ind})\text{Ni}(\text{PPh}_3)_2]^+$ ^{1e} indicated that the formation of undesired byproducts of this type had been circumvented. In addition, the appearance of two different N–Me signals in the ^1H NMR spectrum of the product was consistent with the coordination of the NMe_2 moiety to the nickel center, which is dissymmetric (**2** has C_1 symmetry), and so the $\text{Me}_2\text{N}\rightarrow\text{Ni}$ coordination renders the Me groups diastereotopic. The structural characterization of **2**, which is air stable in the solid state, was completed by an X-ray analysis carried out on a single crystal grown by the slow vapor diffusion of Et_2O into a CH_2Cl_2 solution of this compound. An ORTEP diagram of **2** is shown in Figure 1, along with selected structural parameters. Crystal data and data collection and structure refinement details are given in Table 1. The main features of the structure are described below.

The Ni–N distance of 2.005(2) Å in **2** is within the expected range for $\text{Ni}^{\text{II}}\text{-NR}_3$ bonds,⁵ whereas the Ni–P distance is somewhat longer (by ca. 12σ) than the corresponding distance in the neutral Ni–Cl precursor **1**;⁴ this is likely the result of the steric hindrance caused by the amine moiety. The strain imposed by the chelation of the tether is reflected in the small C1–Ni–N angle of 84.81(10)° (compared to ca. 96° for the C1–Ni–Cl angle in **1**) and the large P–Ni–N angle of 107.52(7)° (compared to ca. 98° for the P–Ni–Cl angle in **1**). The chelation can also be invoked to explain why Ni–C1 is shorter than Ni–C3 despite the greater relative trans influence of PPh_3 , which would otherwise be expected to result in a longer Ni–C1 bond.

The coordination of the indenyl moiety in **2** is intermediate between η^5 and η^3 , as inferred from the significantly shorter Ni–C1, Ni–C2, and Ni–C3 distances compared to Ni–C3A and Ni–C7A. The degree of such “slippage” away from the idealized η^5 coordination is often measured by the parameter $\Delta(\text{M}-\text{C}) = \frac{1}{2}[(\text{M}-\text{C3A} + \text{M}-\text{C7A}) - (\text{M}-\text{C1} + \text{M}-\text{C3})]$,⁶ which is

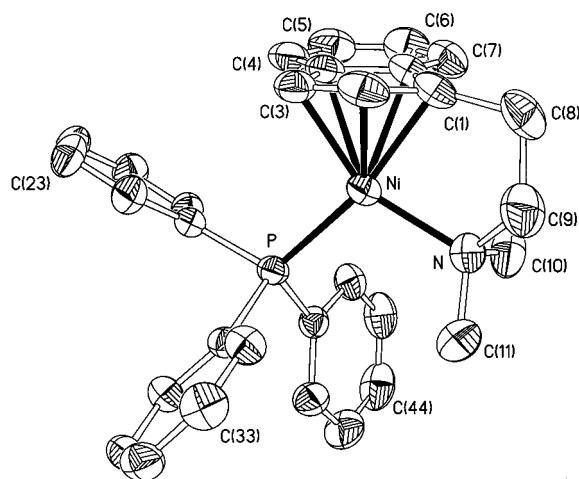


Figure 1. ORTEP view of complex **2**. The counterion and hydrogen atoms are omitted for clarity. Thermal ellipsoids are shown at 40% probability. Selected bond distances (Å) and angles (deg): Ni–P = 2.1971(11), Ni–N = 2.005(2), Ni–C(1) = 2.040(2), Ni–C(2) = 2.056(3), Ni–C(3) = 2.078(3), Ni–C(3A) = 2.327(3), Ni–C(7A) = 2.314(2), C(1)–C(2) = 1.412(4), C(2)–C(3) = 1.399(4), C(3)–C(3A) = 1.455(3), C(3A)–C(7A) = 1.420(3), C(1)–C(7A) = 1.463(3), $\Delta(\text{M}-\text{C}) = 0.26$,⁶ P–Ni–N = 107.52(7), C(3)–Ni–N = 149.55(10), C(3)–Ni–P = 101.79(8), C(1)–Ni–N = 84.86(11), C(1)–Ni–P = 166.49(8), C(1)–Ni–C(3) = 66.97(11). C3A and C7A refer to the atoms shared by the five- and six-membered rings of Ind.

Table 1. Crystal Data and Data Collection and Structure Refinement Details of **2**

formula	$\text{C}_{35}\text{H}_{51}\text{BNPNi}$
mol wt	826.46
cryst color	dark red
cryst habit	block
cryst dimens, mm	$0.36 \times 0.28 \times 0.16$
symmetry	triclinic
space group	$P\bar{1}$
<i>a</i> , Å	11.161(6)
<i>b</i> , Å	14.119(5)
<i>c</i> , Å	15.115(9)
α , deg	82.69(4)
β , deg	79.86(6)
γ , deg	72.65(4)
<i>V</i> , Å ³	2231(2)
<i>Z</i>	2
<i>D</i> (calcd), g cm ^{−3}	1.2303
diffractometer	Nonius CAD-4
temp, K	293(2)
$\lambda(\text{Cu K}\alpha)$, Å	1.540 56
μ , mm ^{−1}	1.240
scan type	$\omega/2\theta$
θ_{max} , deg	69.80
<i>hkl</i> range	$-13 \leq h \leq 13$ $-17 \leq k \leq 17$ $-18 \leq l \leq 18$
no. of rflns used ($I > 2\sigma(I)$)	6134
abs cor	integration ABSORB ¹⁹
<i>T</i> (min, max)	0.6601, 0.8336
$R(F^2) > 2\sigma(F^2)$, $R_w(F^2)$	0.0386, 0.0942
GOF	0.898

0.26 Å for **2**. Interestingly, this degree of slippage is similar to those of the neutral compounds (1-Me-Ind)-(PPh₃)Ni–X (0.25 Å for X = Cl^{1f} and 0.27 Å for X = phthalimide^{1c}) but larger than the $\Delta(\text{M}-\text{C})$ of cationic analogues such as $[(1\text{-Me-Ind})\text{Ni}(\text{PPh}_3)(\text{PMe}_3)]^+$ (0.19

(5) On the basis of 1290 crystal structures of compounds containing a Ni–NR₃ bond (Cambridge Structural Database, version 5.18; Cambridge University: Cambridge, England; accessed Nov 2000), the average and median Ni–NR₃ bond lengths are 2.087 and 2.100 Å, respectively.

(6) (a) Baker, R. T.; Tulip, T. H. *Organometallics* **1986**, *5*, 839. (b) Westcott, S. A.; Kakkar, A.; Stringer, G.; Taylor, N. J.; Marder, T. B. *J. Organomet. Chem.* **1990**, *394*, 777.

Table 2. Polymerization Experiments with $(\eta^3:\eta^0\text{-Ind}(\text{CH}_2)_2\text{NMe}_2)\text{Ni}(\text{PPh}_3)\text{Cl}$ (1**) and $(\eta^3:\eta^1\text{-Ind}(\text{CH}_2)_2\text{NMe}_2)\text{Ni}(\text{PPh}_3)[\text{BPh}_4]$ (**2**)**

run	catalyst	amt of monomer, equiv		T (°C)	time (days)	M_w	M_w/M_n	TON
		styrene	norbornene					
1	2	2000		20	7			0
2	2	2000		80	2	77338	3.2	364
3	2 /AgBF ₄ ^a	2000		80	2	12726	1.9	980
4	2 /AgCl ^a	2000		80	2	65980	1.2	860
5	2		1000	20	4			0
6	2		800	80	4	763	1.1	35
7	2	300	100	50	2	18320	12.0	19
8	2	200	200	50	2	3071	4.5	9
9	2	100	300	50	2	570	1.4	3
10	1 /AgBF ₄ ^a	2000		20	2	1531	1.3	1650
11	1 /AgBF ₄ ^a	2000		60	2	2066	1.5	1570
12	1 /AgBF ₄ ^a		1000	20	2	insol ^b		270
13	1 /AgBF ₄ ^a		1000	60	2	insol ^c		350
14	1 /AgBF ₄ ^a	300	100	50	2	6935	1.4	400
15	1 /AgBF ₄ ^a	200	200	50	2	7184 ^d	1.5	200
16	1 /AgBF ₄ ^a	100	300	50	2	7370 ^e	1.5	300

^a [Ag]/[Ni] = 10. ^b DSC analysis shows exothermic decomposition starting at 300 °C (before mp). ^c DSC analysis shows exothermic decomposition starting at ca. 290 °C (before mp). ^d Partially soluble in THF. DSC analysis shows exothermic decomposition starting at 270 °C (before mp). ^e Slightly soluble in THF. A DSC analysis shows exothermic decomposition starting at 300 °C (before mp).

Å).^{1e} Similar structural parameters have been found in the recently reported Cp analogue $[(\eta^5:\eta^1\text{-Cp}(\text{CH}_2)_2\text{NMe}_2)\text{Ni}(\text{PPh}_3)]^+$,⁷ although there is little distortion in the hapticity of the Cp ligand in this compound.⁸

Catalytic Reactions. The availability of a preformed, stable cationic Ni compound in which one coordination site is occupied by a relatively labile amine moiety (vide infra) presented an opportunity to study the catalytic reactivities of **2**. Mindful of the catalytic activities of a number of cationic Ni(II) complexes in olefin oligomerization and polymerization reactions,⁹ we proceeded to examine the reactivities of complex **2** with alkenes. Our objective was to establish whether the proximity of the amine moiety to the Ni center would have a major influence on the course of the catalysis.

Complex **2** reacted only very sluggishly with styrene at room temperature (run 1, Table 2), implying that the displacement of the amine moiety by styrene is not facile. However, heating the mixture to 80 °C accelerated the polymerization and gave a soluble polystyrene

with $M_w = 77\,338$ and $M_w/M_n = 3.15$, and turnover numbers of ca. 300–400 (run 2, Table 2). The ¹H NMR spectra (CDCl₃) of these polymers show characteristically broad signals at 7.05, 6.59, 1.85, and 1.45 ppm, while the ¹³C{¹H} NMR spectra show broad signals at 145.5 (ipso-C), 128.1 (*o*- and *m*-C), 125.5 (*p*-C), and 43.7 and 40.5 ppm. The analogous reaction with norbornene also requires heating to 80 °C but gives only oligomeric materials ($M_w = 763$; $M_w/M_n = 1.1$) with turnover numbers of 20–40 (runs 5 and 6, Table 2). Attempts at copolymerizing these two olefins were unsuccessful and gave instead polystyrenes only (runs 7–9, Table 2).

It is noteworthy that the outcomes of the reactions of styrene and norbornene with **2** are quite different from the analogous reactions catalyzed by the in situ generated species $[\text{IndNi}(\text{PPh}_3)]^+$. For instance, catalysis by $[\text{IndNi}(\text{PPh}_3)]^+$ proceeds at room temperature to give insoluble norbornene polymers and soluble styrene trimers and tetramers.¹⁰ Moreover, the latter system can catalyze the formation of various styrene–norbornene copolymers. To our surprise, the polymerization reactions catalyzed by the cationic species generated in situ by reacting the precursor complex $(\eta^3:\eta^0\text{-Ind}(\text{CH}_2)_2\text{NMe}_2)(\text{PPh}_3)\text{Ni}-\text{Cl}$ (**1**) with AgBF₄ gave results which were similar to those obtained from in situ generated $[\text{IndNi}(\text{PPh}_3)]^+$ but very different from the results of the polymerizations catalyzed by preformed **2** (compare runs 1 and 2 to runs 10 and 11, runs 5 and 6 to 12 and 13, and runs 7–9 to 14–16; Table 2). We suspect that the difference in the reactivities of **2** and the in situ generated $[\text{IndNi}(\text{PPh}_3)]^+$ results from the influence of the amine tether on the course of the reaction. Thus, when **2** is generated in situ (from **1** and AgBF₄), it is possible that the amine moiety remains coordinated to the unreacted AgBF₄ (or the in situ produced AgCl) and hence cannot exert any influence on the course of the catalysis. This assertion is consistent with the results of experiments which showed that the catalysis with **2**/styrene in the presence of added AgBF₄ (run 3, Table 2) gave results intermediate between the catalysis with **2**/styrene and that with **1**/AgBF₄/styrene (runs 2 and 10, Table 2). Added AgCl had no influence in the catalysis, probably because of its poor solubility (run 4, Table 2). We believe that these results indicate that the amine moiety in these complexes plays an important role in modulating these catalytic reactions. It should be noted, however, that the observed differences in the outcomes of the polymerizations catalyzed by **2** and **1**/AgBF₄ might also be due to the presence of some side products generated in the latter system.¹¹

Another catalytic reaction which was studied briefly is the dehydrogenative oligomerization of PhSiH₃. Complex **2** was found to catalyze the dimerization of PhSiH₃ at room temperature to give PhH₂Si–SiPhH₂ in ca. 20 turnovers as well as small amounts of the trimer and tetramers.¹² As was the case for the reactions of styrene and norbornene, here too the outcome of the catalysis

(10) Fontaine, F.-G.; Dubois, M.-A.; Zargarian, D. Unpublished results.

(11) (a) We thank one of the reviewers for pointing out this possibility. (b) It should be noted that styrene can be polymerized by Ag⁺ (Hermans, J. P.; Smets, G. *J. Polym. Sci., Part A* **1965**, *3*, 3175), but this reaction is much slower than that catalyzed by the **1**/AgBF₄ and requires higher temperatures (above 70 °C).

(7) Segnitz, O.; Winter, M.; Merz, K.; Fisher, R. *Eur. J. Inorg. Chem.* **2000**, 2077.

(8) For a detailed study on the hapticity in the analogous Ni(Cp) complexes see: Holland, P. L.; Smith, M. E.; Andersen, R. A.; Bergman, R. G. *J. Am. Chem. Soc.* **1997**, *119*, 12815.

(9) (a) Johnson, L. K.; Killian, C. M.; Arthur, S. D.; Feldman, J.; McCord, E. F.; McLain, S. J.; Kreutzer, K. A.; Bennett, M. A.; Coughlin, E. B.; Httel, S. D.; Parthasarathy, A.; Tempel, D. J.; Brookhart, M. S.; DuPont, WO 96/23010, 1996. (b) Johnson, L. K.; Killian, C. M.; Brookhart, M. S. *J. Am. Chem. Soc.* **1995**, *117*, 6414. (c) Keim, W.; Appel, R.; Gruppe, S.; Knoch, F. *Angew. Chem.* **1987**, *99*, 1042. (d) Ostojka-Starzewski, K. A.; Witte, J. *Angew. Chem.* **1985**, *97*, 610. (e) Flid, V. R.; Kuznetsov, V. B.; Grigor'ev, A. A.; Belov, A. P. *Kinet. Catal.* **2000**, *41*(5), 604. (f) Flid, V. R.; Manulik, O. S.; Grigor'ev, A. A.; Belov, A. P. *Kinet. Catal.* **2000**, *41*(5), 658. (g) Goodall, B. L.; Benedikt, G. M.; McIntosh, L. H.; Barnes, D. A. U.S. Patent 5,468,819, 1995. (h) Goodall, B. L.; Benedikt, G. M.; McIntosh, L. H.; Barnes, D. A.; Rhodes, L. F. U.S. Patent 5,468,819, 1995. (i) Bonnet, M. C.; Dahan, F.; Ecker, A.; Keim, W.; Schulz, R. P.; Tkatchenko, I. *J. Chem. Soc., Chem. Commun.* **1994**, 615. (j) Aresta, M.; Dibenedetto, A.; Quaranta, E.; Lanfanchi, M.; Tiripicchio, A. *Organometallics* **2000**, *19*, 4199. (k) Ihara, E.; Fujimura, T.; Yasuda, H.; Maruo, T.; Kanehisa, N.; Kai, Y. *J. Polym. Sci., Part A: Polym. Chem.* **2000**, *38*, 4764.

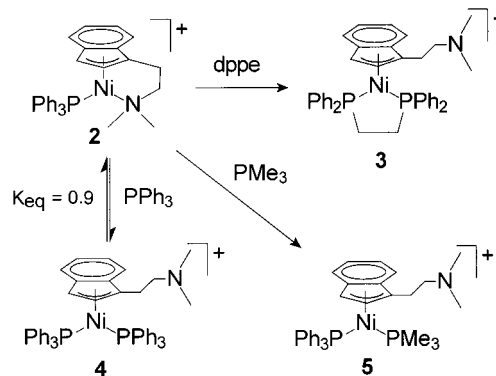
by **2** is qualitatively different from the analogous reaction catalyzed by the in situ generated cation, which gives $(\text{PhSiH})_n$ consisting of both cyclic ($M_n = \text{ca. } 600$) and linear ($M_n = \text{ca. } 1500$) oligomers.^{1d} At this stage, we speculate that the dehydrogenative oligomerization of PhSiH_3 catalyzed by **2** does not proceed beyond dimerization because the dimer produced in the initial Si–Si bond formation step cannot compete effectively with the NMe_2 moiety for coordination to Ni. In contrast to the case with the olefin polymerizations, the combination of $(\eta^3:\eta^0\text{-Ind}(\text{CH}_2)_2\text{NMe}_2)(\text{PPh}_3)\text{Ni-Cl}$ and AgBF_4 did not catalyze the oligomerization of PhSiH_3 .

The above results indicated that the strength of the coordination of the amine tether to the Ni center can determine the ease with which the catalytic reactions may be initiated (e.g., requirement for heating) and can affect the overall outcome of the reactions (e.g., oligomerization vs polymerization). To evaluate the binding strength of the amine tether, we have studied the reaction of complex **2** with various neutral and anionic ligands, as follows.

Ligand Substitution Reactions with Neutral Lewis Bases. No reaction was observed between **2** and CO even with a 25 psi pressure of CO, but phosphines and some amines did react to displace the amine tether to varying degrees. Thus, only 1 equiv of bis(diphenylphosphino)ethane (dppe) was sufficient to displace both the amine tether and the PPh_3 ligand in **2**, giving an orange-red powder. Recrystallization of this material from $\text{Et}_2\text{O}/\text{CH}_2\text{Cl}_2$ gave, in ca. 64% yield, the complex $[(\eta^3:\eta^0\text{-Ind}(\text{CH}_2)_2\text{NMe}_2)\text{Ni}(\text{dppe})][\text{BPh}_4]$ (**3**), whose identity was confirmed by elemental analysis and NMR spectroscopy. The absence of a C_2 axis in **3** renders the two P nuclei of the dppe ligand inequivalent, and so the $^{31}\text{P}\{^1\text{H}\}$ NMR spectrum displays two broad signals at 65.6 and 68.7 ppm at room temperature. At -40°C , the two signals appear as sharp doublets at 66.4 and 70.8 ppm ($^2J_{\text{P-P}} = 25.4$ Hz), whereas warming to 35°C brings about coalescence (broad signal at 66.6 ppm); an energy barrier of 14.3 kcal mol $^{-1}$ was calculated for this process using the Holmes–Gutowski equation.¹³ Similar dynamic exchange processes have been observed for other complexes of this family and are attributed to the hindered rotation of the indenyl moiety.^{1e,h}

In contrast to the facile reaction with dppe, disruption of the N→Ni chelation in **2** by PPh_3 is much less favorable thermodynamically and requires a large excess of PPh_3 . The reaction can be monitored by the emergence in the $^{31}\text{P}\{^1\text{H}\}$ NMR spectrum of a new set of AB resonances at 32.3 and 36.1 ppm ($^2J_{\text{P-P}} = 27$ Hz). These signals are very similar to those reported^{1d} for $[(1\text{-Me-Ind})\text{Ni}(\text{PPh}_3)_2]^+$ (cf. 32.5 and 35.8 ppm, $^2J_{\text{P-P}} = 25$ Hz), and so the product of this reaction is proposed to be $[(\eta^3:\eta^0\text{-Ind}(\text{CH}_2)_2\text{NMe}_2)\text{Ni}(\text{PPh}_3)_2][\text{BPh}_4]$ (**4**). Separation and isolation of pure **4** has not been possible because of the small K_{eq} value of ca. 0.9 for this reaction (Scheme 3).

Scheme 3. Reactivity of **2** with Phosphines



The reaction of **2** with PMe_3 was less straightforward, and its outcome depended on the relative amount of PMe_3 present in the reaction medium. For instance, reacting **2** with an excess of PMe_3 gave free PPh_3 and $\text{Ni}(\text{PMe}_3)_4$ as the major products, whereas the reaction with 1 equiv of PMe_3 gave, in addition to free PPh_3 and small amounts of $\text{Ni}(\text{PMe}_3)_4$, two new species with the following spectral features (Table 4): the major species displayed an AX set of doublets at -10.9 and 41.0 ppm for PMe_3 and PPh_3 , respectively ($^2J_{\text{P-P}} = 42$ Hz), while the minor product gave a singlet at -16.6 ppm in $^{31}\text{P}\{^1\text{H}\}$ NMR spectroscopy. The AX resonances are virtually identical with the signals displayed by the known^{1e} bis(phosphine) compound $[(1\text{-Me-Ind})\text{Ni}(\text{PPh}_3)(\text{PMe}_3)]^+$ (cf. -10.1 and 41.2 ppm and $^2J_{\text{P-P}} = 42$ Hz for one rotamer),¹⁵ and so we propose that the major product of the reaction of 1 equiv of PMe_3 with **2** is $[(\eta^3:\eta^0\text{-Ind}(\text{CH}_2)_2\text{NMe}_2)\text{Ni}(\text{PPh}_3)(\text{PMe}_3)][\text{BPh}_4]$ (**5**). The minor product is presumably the complex $[(\eta^3:\eta^1\text{-Ind}(\text{CH}_2)_2\text{NMe}_2)\text{Ni}(\text{PMe}_3)]^+$, arising from the displacement of the PPh_3 from **2** by PMe_3 . These assignments are somewhat tentative, however, because all attempts at separation and isolation of these products have resulted in the formation of intractable materials, thus preventing their conclusive characterization.

The reaction of **2** with primary and secondary amines such as H_2NET , HNET_2 , aniline, and $\text{H}_2\text{N}(t\text{-Bu})$ gave complex mixtures of products (by ^1H NMR) in which the only P-containing species was free PPh_3 (by $^{31}\text{P}\{^1\text{H}\}$ NMR) and from which no tractable compounds could be isolated. Tertiary amines such as NET_3 do not react at all with **2**, even in a large excess, but pyridine and its methyl-substituted analogues showed reactivities similar to that observed with PPh_3 (Scheme 4). As was the case with PPh_3 , we were unable to isolate the new compounds because removal of the excess ligand during isolation re-formed **2**; nevertheless, the identity of the products can be ascertained from the following NMR data. The ^1H NMR spectra of the mixtures of **2** and the pyridines indicated the formation of a new compound in equilibrium with **2**. The signals arising from the Ind protons in the new compound were very similar to those

(12) These products were identified on the basis of their characteristic ^1H NMR signals as reported in: (a) Gauvin, F. Ph.D. Thesis, McGill University, Montréal, Québec, Canada, 1992. (b) Aitken, C.; Barry, J.-P.; Gauvin, F.; Harrod, J. F.; Malek, A.; Rousseau, D. *Organometallics* **1989**, *8*, 1732.

(13) (a) $\Delta G^\ddagger = RT[\ln(22.96 + \ln(T/\Delta\delta))]$. (b) Abraham, R. J.; Loftus, P. *Proton and Carbon-13 NMR Spectroscopy: an Integrated Approach*; Wiley: Toronto, 1985; pp 165–168.

(14) This compound is identified by its singlet resonance (at ca. -21.5 ppm) in the $^{31}\text{P}\{^1\text{H}\}$ NMR spectrum: Tolman, C. A.; Seidel, W. C.; Gosser, L. W. *J. Am. Chem. Soc.* **1974**, *96*, 53.

(15) It is interesting to note that the $^{31}\text{P}\{^1\text{H}\}$ spectrum of $[(1\text{-Me-Ind})\text{Ni}(\text{PPh}_3)(\text{PMe}_3)]^+$ shows two sets of signals (AX and AX') attributed to the nonequivalent rotamers arising from the hindered rotation of the indenyl ring,^{1d} whereas compound **5** shows only one set of signals at room temperature, presumably because of a higher rotational barrier.

Scheme 4. Equilibrium Reaction of **2** with Pyridine and Pyridine Analogues

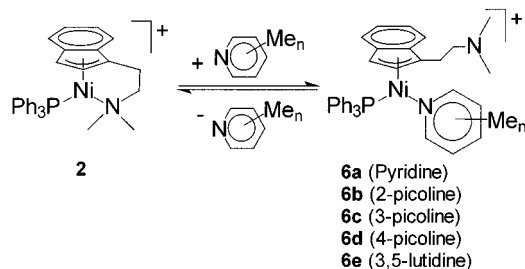


Table 3. Spectroscopic Data and Equilibrium Constants of $[(\eta^3:\eta^0\text{-Ind}(\text{CH}_2)_2\text{NMe}_2)\text{Ni}(\text{PPh}_3)(\text{L})][\text{BPh}_4]$

L	$^{31}\text{P}\{^1\text{H}\}$ (ppm)	^1H (ppm)			K_{eq}
		H2	H3	NMe ₂	
6a pyridine	32.13	6.28	4.18	2.14	9 ± 1
6b 2-picoline	28.76	6.38	4.07	2.07	2.0 ± 0.2
6c 3-picoline	32.15	6.35	4.17	2.14	23 ± 2
6d 4-picoline	32.06	6.28	4.15	2.04	33 ± 3
6e 3,5-lutidine	32.03	6.39	4.15	2.11	16 ± 1

of **2**, whereas the signals for the protons on the tether were broadened as a result of the exchange reaction. Significantly, a new singlet at ca. 2.1 ppm replaced the previously inequivalent N–Me resonances at 1.6 and 1.3 ppm. The $^{31}\text{P}\{^1\text{H}\}$ NMR spectra of the mixtures of **2** and the pyridines showed the conversion of **2** to new derivatives which displayed a singlet resonance at ca. 32 ppm for all but one case; the corresponding signal for the reaction with 2-picoline appeared at ca. 29 ppm. These observations are consistent with the formation of the cations $[(\eta^3:\eta^0\text{-Ind}(\text{CH}_2)_2\text{NMe}_2)\text{Ni}(\text{PPh}_3)(\text{L})][\text{BPh}_4]$ (**6**; Table 3), which arise from the displacement of the tether in **2**. The more upfield $^{31}\text{P}\{^1\text{H}\}$ signal in the 2-picoline derivative **6b** implies a less efficient $\text{PPh}_3\text{-Ni}$ donation due to larger steric interactions between PPh_3 and 2-picoline. The equilibrium constants for these exchange reactions were determined to be 33 (4-picoline), 23 (3-picoline), 16 (3,5-lutidine), 9 (pyridine), and 2.0 (2-picoline). The relative values of K_{eq} reflect the sensitivity of this ligand substitution reaction to both steric and electronic factors: pyridine > 2-picoline (steric factor); 4-picoline > 3-picoline > 3,5-lutidine > pyridine (electronic factor).

Reactivities of **2 with Anionic Ligands.** The anionic nucleophiles Ph_2P^- , Me_2N^- , and Me^- did not show any reactivity with **2** in Et_2O and THF, presumably because of the limited solubility of **2** in these solvents. Even in CH_2Cl_2 , in which it is soluble, **2** did not react with Cl^- or Br^- but reaction with a large excess of LiI resulted in the formation of a red powder which was crystallized from $\text{CH}_2\text{Cl}_2/\text{hexane}/\text{Et}_2\text{O}$ to give $(\eta^3:\eta^0\text{-Ind}(\text{CH}_2)_2\text{NMe}_2)(\text{PPh}_3)\text{Ni-I}\cdot\text{LiBPh}_4$ (**7**) in 84% yield.¹⁶ Complex **7** has been characterized completely, including a single-crystal X-ray analysis. The ^1H NMR spectrum of this compound was very similar to that of **1**, and the $^{31}\text{P}\{^1\text{H}\}$ NMR showed a singlet at 35.9 ppm (Table 4). The X-ray data we have obtained for complex **7** confirmed the connectivity, but the poor quality of the crystals, the significant absorption of the $\text{Cu K}\alpha$ radi-

ation by iodine atoms, and the presence of $\text{LiBPh}_4\cdot\text{H}_2\text{O}$ in the crystal lattice prevented us from refining the structure to a satisfactory level.

Conclusion. The results of the ligand substitution reactions described above show that the coordination of the tether in **2** is strong enough to stabilize this compound and prevent the formation of the catalytically inert complex $[(\eta^3:\eta^0\text{-Ind}(\text{CH}_2)_2\text{NMe}_2)\text{Ni}(\text{PPh}_3)_2]^+$ yet labile enough to be displaced by relatively strong ligands. Thus, the amine tether in complex **1** can act as a hemilabile ligand which can stabilize cationic species such as **2** while allowing the coordination of some ligands and substrates. This property facilitates the use of complex **2** as a single-component precatalyst for the polymerization of styrene, oligomerization of norbornene, and dimerization of PhSiH_3 . Comparisons with the analogous reactions catalyzed by cations generated in situ from $(1\text{-Me-Ind})(\text{PPh}_3)\text{Ni-Cl}$ and $(\eta^3:\eta^0\text{-Ind}(\text{CH}_2)_2\text{NMe}_2)(\text{PPh}_3)\text{Ni-Cl}$ indicate that the presence of the amine tether has a marked influence on the course of the catalysis. Future studies will investigate the reactivity of **2** with ethylene and other olefins, and will focus on understanding the role of the amine tether in the catalysis.

Experimental Section

General Comments. All manipulations, except for the GPC and DSC analyses, were performed under an inert atmosphere of N_2 or argon using standard Schlenk techniques and a drybox. Dry, oxygen-free solvents were employed throughout. The syntheses of **1** and **2** have been reported previously.⁴ LiPPh_2 and LiNMe_2 were prepared by deprotonation of HPPH_2 and HNMe_2 , respectively; all other reagents used in the experiments were obtained from commercial sources and used as received. The elemental analyses were performed by the Laboratoire d'analyse élémentaire (Université de Montréal). The spectrometers used for recording the NMR spectra are as follows: Bruker AMXR400 (^1H (400 MHz), $^{13}\text{C}\{^1\text{H}\}$ (100.56 MHz), and $^{31}\text{P}\{^1\text{H}\}$ (161.92 MHz)), and Bruker AV300 (^1H (300 MHz) and $^{31}\text{P}\{^1\text{H}\}$ (121.49 MHz)).

Crystal Structure Determinations. Dark red crystals of **2** were obtained at room temperature by the slow diffusion of Et_2O vapor into a CH_2Cl_2 solution of **2**. The crystal data for **2** were collected on a Nonius CAD-4 diffractometer with graphite-monochromated $\text{Cu K}\alpha$ radiation at 293(2) K using CAD-4 software. The refinement of the cell parameters was done with the CAD-4 software,¹⁸ and the data reduction used NRC-2 and NRC-2A.¹⁹ The structure was solved by direct methods using SHELXS97²⁰ and difmap synthesis using SHELXL96;²¹ the refinements were done on F^2 by full-matrix least squares. All non-hydrogen atoms were refined anisotropically, while the hydrogens (isotropic) were constrained to the parent atom using a riding model. Crystal data and experimental details for **2** are listed in Table 1, and selected bond distances and angles are listed under the ORTEP diagram.

Polymerization of Styrene. Runs 1 and 2. **2** (18 mg) and styrene (4.5 g, 2000 equiv.) were stirred for 7 days in CH_2Cl_2 (8 mL) at room temperature (run 1) or for 2 days at 80 °C (run

(17) Dubois, M.-A. M.Sc. Thesis, Université de Montréal, Montréal, Québec, Canada, 1999.

(18) CAD-4 Software, Version 5.0; Enraf-Nonius, Delft, The Netherlands, 1989.

(19) Gabe, E. J.; Le Page, Y.; Charlant, J.-P.; Lee, F. L.; White, P. S. *J. Appl. Crystallogr.* **1989**, *22*, 384.

(20) Sheldrick, G. M. SHELXS: Program for the Solution of Crystal Structures; University of Göttingen, Göttingen, Germany, 1997.

(21) Sheldrick, G. M. SHELXL: Program for the Refinement of Crystal Structures; University of Göttingen, Göttingen, Germany, 1996.

(16) The analogous Cp derivative has been reported without characterization data: Nlate, S.; Herdweck, E.; Fischer, R. A. *Angew. Chem., Int. Ed. Engl.* **1996**, *35*, 1861.

Table 4. $^{31}\text{P}\{^1\text{H}\}$ NMR Data of Complexes 1–7

compd	no.	δ (ppm) ^a	$^2J_{\text{P-P}}$ (Hz)	ref
$(\eta^3\text{:}\eta^0\text{-Ind}(\text{CH}_2)_2\text{NMe}_2)\text{Ni}(\text{PPh}_3)\text{Cl}$	1	30.8 ^b		4
$[(\eta^3\text{:}\eta^1\text{-Ind}(\text{CH}_2)_2\text{NMe}_2)\text{Ni}(\text{PPh}_3)]\text{[BPh}_4]$	2	29.1		4
$[(\eta^3\text{:}\eta^0\text{-Ind}(\text{CH}_2)_2\text{NMe}_2)\text{Ni}(\text{dppe})]\text{[BPh}_4]$	3	70.8, 66.4 ^c	25.4 ^c	
$[(\eta^3\text{:}\eta^0\text{-Ind}(\text{CH}_2)_2\text{NMe}_2)\text{Ni}(\text{PPh}_3)(\text{PMe}_3)]\text{[BPh}_4]$	4	41.0, -10.9	42	
$[(1\text{-Me-Ind})\text{Ni}(\text{PPh}_3)(\text{PMe}_3)]\text{[BPh}_4]$		41.2, -10.1	42	1e
$[(\eta^3\text{:}\eta^0\text{-Ind}(\text{CH}_2)_2\text{NMe}_2)\text{Ni}(\text{PPh}_3)_2]\text{[BPh}_4]$	5	36.1, 32.3	27	
$[(1\text{-Me-Ind})\text{Ni}(\text{PPh}_3)_2]\text{[BPh}_4]$		32.5, 35.8	25	1e
$[(\eta^3\text{:}\eta^0\text{-Ind}(\text{CH}_2)_2\text{NMe}_2)\text{Ni}(\text{PPh}_3)(\text{Py})]\text{[BPh}_4]$	6a	32.1		
$(\eta^3\text{:}\eta^0\text{-Ind}(\text{CH}_2)_2\text{NMe}_2)\text{Ni}(\text{PPh}_3)\text{I.LiBPh}_4$	7	35.9		
$(1\text{-Me-Ind})\text{Ni}(\text{PPh}_3)\text{I}$		38.6 ^b		17

^a Unless otherwise stated, all spectra are run in CDCl_3 at room temperature. ^b C_6D_6 . ^c At -40°C .

2). For run 1, removal of the solvent and unreacted styrene gave a thin film which was washed with CDCl_3 and analyzed by ^1H NMR spectroscopy, showing broad peaks of polystyrene. For run 2, removal of solvent and unreacted styrene gave a light gray solid (829 mg, 18% yield), which was isolated and analyzed by GPC (THF; $M_w = 77\,338$; $M_w/M_n = 3.15$) and NMR spectroscopy. ^1H NMR (CDCl_3): δ 7.05 (br), 6.59 (br), 1.85 (br), 1.45 (br). $^{13}\text{C}\{^1\text{H}\}$ (CDCl_3): δ 145.5 (*ipso-C*), 128.1 (*o*- and *m*-C), 125.5 (*p*-C), 43.7 and 40.5 (alkyl chain).

Runs 3 and 4. **2** (15 mg), styrene (3.8 g, 2000 equiv), and AgCl (26 mg, run 3) or AgBF_4 (35 mg, run 4) were stirred for 2 days in CH_2Cl_2 (8 mL) at 80°C . Removal of the solvent and unreacted styrene gave a thick gray oil, which was isolated and analyzed by GPC (run 3, 1.7 g, 43% yield, GPC (THF) $M_w = 65\,980$, $M_w/M_n = 1.2$; run 4, 1.9 g, 49% yield, GPC (THF) $M_w = 12\,726$; $M_w/M_n = 1.9$).

Runs 10 and 11. Styrene (8.3 g, 2000 equiv) and CH_2Cl_2 (8 mL) were syringed into a mixture of **1** (22 mg) and AgBF_4 (85 mg, 10 equiv). The solution was stirred for 2 days at room temperature (run 10) or at 60°C (run 11). Removal of the solvent and the unreacted styrene under vacuum gave polystyrene (run 10, thick oil, 6.9 g, 83% yield; run 11, sticky solid, 9.0 g, 79% yield), which was analyzed by GPC (THF; run 10, $M_w = 1531$, $M_w/M_n = 1.29$; run 11, $M_w = 2066$, $M_w/M_n = 1.48$).

Polymerization of Norbornene. Runs 5 and 6. **2** (ca. 19 mg) and norbornene (ca. 2.3 g, 1000 equiv) were stirred in CH_2Cl_2 (3 mL) for 4 days at room temperature (run 5) or at 80°C (run 6). Removal of the solvent and unreacted norbornene left only unreacted **2** (run 5) or a gray solid (run 6, 101 mg, 4.4% yield), which was analyzed by GPC (THF; $M_w = 763$; $M_w/M_n = 1.1$).

Runs 12 and 13. CH_2Cl_2 (8 mL) is added to **1** (ca. 23 mg), AgBF_4 (ca. 80 mg, 10 equiv), and norbornene (ca. 4.0 g, 1000 equiv). A white solid precipitated immediately after the addition of the solvent. After 2 days at room temperature (run 12) or at 60°C (run 13), a gray insoluble solid (run 12, 1.1 g, 27% yield; run 13, 1.2 g, 35% yield) was obtained. Thermal analysis (DSC) of the polymers showed an exothermic decomposition starting at 300°C , giving a black powder after the analysis.

Copolymerization of Styrene and Norbornene. Runs 7–9. **2** (ca. 20 mg) was reacted with styrene and norbornene (with ratios of 300:100 (run 7), 200:200 (run 8), and 100:300 (run 9)) for 2 days in CH_2Cl_2 (2 mL) at 50°C . The solvent and the unreacted monomers were then removed under vacuum to give a thick oil, which was isolated (yields ca. 5% (run 7), 2% (run 8), and 1% (run 9)) and analyzed by ^1H NMR spectroscopy and GPC (THF). Integration of the alkane vs aromatic protons in the ^1H NMR spectra showed that the product obtained was polystyrene.

Runs 14–16. Stirring **1** (ca. 18 mg) and AgBF_4 (ca. 65 mg) with mixtures of styrene and norbornene (with ratios of 300:100 (run 14), 200:200 (run 15), and 100:300 (Run 16)) for 3 days in CH_2Cl_2 (3 mL) at 50°C gave, after removal of solvent and unreacted monomers, a gray solid, which was isolated (yields: run 14, >95%; run 15, 75%; run 16, 56%) and analyzed by ^1H NMR spectroscopy, GPC, and DSC (runs 15 and 16).

The results are presented in Table 2. Integration of alkane vs aromatic protons in ^1H NMR spectroscopy showed that copolymers were formed that kept the starting proportion of styrene and norbornene. The results of the GPC analyses (in THF) were as follows: run 14, totally soluble, $M_w = 6935$, $M_w/M_n = 1.4$; run 15, partially soluble, $M_w = 7184$, $M_w/M_n = 1.5$; run 16, slightly soluble, $M_w = 7370$, $M_w/M_n = 1.5$. Thermal analysis of the solids obtained from runs 15 and 16 showed exothermic degradations of the polymers (at ca. 300°C), giving a black powder after the analysis.

Dehydropolymerization of Phenylsilane. Into a vessel containing **1** (ca. 15 mg) and AgBF_4 (ca. 55 mg, 10 equiv) was syringed a CH_2Cl_2 solution (3 mL) containing PhSiH_3 (ca. 600 mg, 200 equiv) and the mixture stirred for 3 days at room temperature or at 80°C . Removal of the solvent and the remaining PhSiH_3 gave a black oil, which was analyzed by ^1H NMR spectroscopy. None of the signals characteristic¹² of $(\text{PhSiH}_2)_2$ or the $(\text{PhSiH})_n$ oligomers were detected. **2** (25.8 mg, 0.031 mmol) and PhSiH_3 (676 mg, 6.25 mmol) were stirred for 3 days in CH_2Cl_2 (2 mL) at room temperature. Removal of the volatiles gave a colorless oil, which was analyzed by ^1H NMR spectroscopy. Signals characteristic¹² of the dimer (the major product, 4.49 ppm) and the trimer and tetramer (broad signals at 4.56 ppm) were detected, while the signals for linear or cyclic polymers were absent.

$[(\eta^3\text{:}\eta^0\text{-Ind}(\text{CH}_2)_2\text{NMe}_2)\text{Ni}(\text{dppe})]\text{[BPh}_4]$ (3**).** Overnight stirring of a CH_2Cl_2 (15 mL) mixture of **2** (415 mg, 0.503 mmol) and dppe (201 mg, 0.505 mmol), followed by removal of the solvent, gave a red-orange solid. Two recrystallizations from CH_2Cl_2 and Et_2O (1:10) gave an orange powder (309 mg, 0.32 mmol, 64% yield). $^{31}\text{P}\{^1\text{H}\}$ NMR (CDCl_3): δ 68.66 (br) and 65.65 (br). ^1H NMR (CDCl_3): δ 7.15 and 6.96 (t, H5 and H6), 7.6 to 6.7 (m, $-\text{PPh}_2$, BPh_4), 6.53 (br d, J 8.1 Hz, H4 or H7), 6.02 (br, H2), 5.92 (d, J = 8.2 Hz, H4 or H7), 5.31 (d, J = 2.8 Hz, H3), 2.24 (m, Ind-CH_2-), 2.03 (s, NMe_2), 1.90 (m, $-\text{CH}_2-\text{N}$), 1.69 (m, $-\text{CH}_2\text{P}$). $^{13}\text{C}\{^1\text{H}\}$ NMR (CDCl_3): δ 163.5 (4-line multiplet, $J_{\text{B-C}} = 48$ Hz, *i*-C of BPh_4), 136.4 (*m*-C of BPh_4), 133.3 (d, $^2J_{\text{P-C}} = 8$ Hz, *o*-C of PPh_2), 132.2 (*p*-C of PPh_2), 129.6 (d, $^3J_{\text{P-C}} = 11$ Hz, *m*-C of PPh_2), 128.0 and 127.8 (C5/C6), 125.64 (*o*-C of BPh_4), 121.7 (*p*-C of BPh_4), 119.7 (d, $J_{\text{P-C}} = 9$ Hz, C1), 118.3 and 118.0 (C4/C7), 101.5 (C2), 79.8 (C3), 58.8 (CH_2N), 45.2 (NMe), 30.6 and 27.6 (br m, PCH_2), 24.6 (Ind-CH_2). Anal. Calcd for $\text{C}_{63}\text{H}_{60}\text{P}_2\text{NiBN}\cdot\text{CH}_2\text{Cl}_2$: C, 73.38; H, 5.96; N, 1.34. Found: C, 73.05; H, 6.03; N, 1.23.

Reaction of **2 with PPh_3 .** The ^1H and $^{31}\text{P}\{^1\text{H}\}$ NMR spectra of a CDCl_3 solution of **2** (18.5 mg, 0.022 mmol) and PPh_3 (95 mg, 0.36 mmol) showed the emergence of a new species. ^1H NMR: δ 7.0–7.9 (br m, aromatic signals of PPh_3 , BPh_4 , and Ind), 6.81 (H2), 6.37 (d, $^3J_{\text{H-H}} = 7.6$ Hz, H4 or H7), 6.08 (d, $^3J_{\text{H-H}} = 7.0$ Hz, H4 or H7), 4.94 (H3), 2.11 (NMe_2); broad signals for Ind-CH_2 and CH_2N protons of the new species and of **2** are overlapping. $^{31}\text{P}\{^1\text{H}\}$ NMR δ 35.9 and 32.1 (d, $^2J_{\text{P-P}} = 27$ Hz, PPh_3). The new signals are attributed to the complex $[(\eta^3\text{:}\eta^0\text{-Ind}(\text{CH}_2)_2\text{NMe}_2)\text{Ni}(\text{PPh}_3)_2]\text{[BPh}_4]$ (**4**). A 1:3 mixture of **4** and **2** was ascertained from the integration of the respective signals. Additional PPh_3 (0.37 mmol, 97 mg) was then added to the solution, and the NMR spectra were recorded

15 min later, showing a 1:1 ratio. Removal of the solvent and washing with Et₂O gave a reddish solid, the ³¹P NMR spectrum of which shows only a small signal for **2** and traces of unknown compounds.

Reaction of 2 with PMe₃. PMe₃ (28.5 μ L, 0.28 mmol) was transferred to a stirred solution of **1** (230 mg, 0.28 mmol) in 7 mL of CH₂Cl₂. Analysis of the resulting red solution by ³¹P{¹H} NMR spectroscopy showed the presence of a few species (CDCl₃): δ 41.1 (d, ²J_{P-P} = 42, PPh₃), -10.8 (d, ²J_{P-P} = 42 Hz, PMe₃), 29.5 (s, unreacted **2**), 16.5 (s), -4.5 (s, free PPh₃), -21.5 (s, Ni(PMe₃)₄). The signals at δ 41.1 and -10.8 are attributed to [(η^3 : η^0 -Ind(CH₂)₂NMe₂)Ni(PPh₃)(PMe₃)](BPh₄) (**5**). Removal of the solvent gave a red powder consisting mainly of **2** (187 mg, 20.1 mmol, 71% crude yield).

[(η^3 : η^0 -Ind(CH₂)₂NMe₂)Ni(PPh₃)(Py)](BPh₄) (6a**) in Equilibrium with **2**.** Compound **2** (19.3 mg, 0.023 mmol) and pyridine (13.8 μ L, 0.17 mmol) were mixed together in CDCl₃ and the ¹H and ³¹P{¹H} NMR spectra recorded 15 min later, showing a 2:1 ratio of **6a** and **2** on the basis of the integration of the ³¹P{¹H} NMR signals. ¹H NMR (CDCl₃): δ 8.6–6.8 (m, aromatic protons of PPh₃, Ind, and pyridine), 6.60 and 6.52 (H4/H7), 6.28 (br, H2), 4.18 (s, H3), 2.14 (s, NMe₂); the signals for Ind-CH₂ and CH₂N of **6a** and **2** are overlapping. ³¹P{¹H} NMR (CDCl₃): δ 32.2 (s).

More pyridine (13.8 μ L, 0.17 mmol) was then added to the above sample, and the NMR spectra were recorded 15 min later, showing a 5:1 ratio of **6a** and **2**. Removal of volatiles under vacuum gave a red solid, which was identified as **2** by ³¹P{¹H} and ¹H NMR spectroscopy. The equilibrium constants have been calculated using data obtained from these two sets of measurements at different concentrations; the integrals of the signals for **2** and **6a** in the ¹H (signal for H3) and ³¹P{¹H} NMR spectra were used for the calculations and gave the same results within experimental error (see the Supporting Information).

[(η^3 : η^0 -Ind(CH₂)₂NMe₂)Ni(PPh₃)(L)](BPh₄) (6b–e**) in Equilibrium with **2**. General Procedure.** To a CDCl₃ (ca. 0.75 mL) solution of **2** (ca. 20 mg) was added ca. 5–10 μ L of L (2-picoline, 3-picoline, 4-picoline, 3,5-lutidine), and the NMR spectra were recorded 20 min later. This operation was repeated once or twice with additional aliquots of L. Equilib-

rium constants were derived as explained for **6a** and are tabulated in Table 3, together with the spectroscopic data.

[(η^3 : η^0 -Ind(CH₂)₂NMe₂)Ni(PPh₃)I]·LiBPh₄ (7**).** Compound **2** (508 mg, 0.615 mmol) and LiI (1.6 g, 12.3 mmol) were stirred for 2 h in CH₂Cl₂ (15 mL), and the mixture was then filtered. Evaporation of the filtrate gave a red powder of crude **7**, which was dissolved in 4 mL of CH₂Cl₂ and precipitated by addition of a 1:1 solution of hexane and Et₂O to give the pure product as a red powder (497 mg, 0.518 mmol, 84% yield). ³¹P{¹H} NMR (CDCl₃): δ 35.94. ¹H NMR (CDCl₃): δ 7.6–6.7 (m, BPh₄, PPh₃, aromatic proton of Ind), 6.24 (d, ³J_{H-H} = 5.2 Hz, H4), 6.11 (s, H2), 4.05 (m, H3), 2.50 (m, Ind-CH₂-), 2.17 (m, -CH₂-N), 2.03 (s, NMe₂). ¹³C{¹H} NMR (C₆D₆): δ 164.2 (4-line multiplet, J_{B-C} = 42 Hz, *i*-C of BPh₄), 136.1 (*m*-C of BPh₄), 135.4 (d, ²J_{P-C} = 9 Hz, *o*-C of PPh₃), 132.9 and 132.1 (C3A/C7A), 130.7 (*p*-C of PPh₃), 128.4 (d, ³J_{P-C} = 9 Hz, *m*-C of PPh₃), 128.8 and 127.4 (C5/C6), 126.3 (*o*-C of BPh₄), 122.4 (*p*-C of BPh₄), 118.4 & 117.5 (C4/C7), 101.1 (d, ²J_{P-C} = 25 Hz, C1), 95.2 (C2), 75.1 (C3), 55.8 (CH₂N), 43.51 (NMe), 23.2 (IndCH₂). Anal. Calcd for C₅₅H₅₁LiBNPNIi: C, 68.79; H, 5.35; N, 1.46. Found: C, 68.23; H, 4.90; N, 1.58.

Acknowledgment. Francine Bélanger-Gariépy and Ernesto Rivera-Garcia are gratefully acknowledged for their help with the crystallography and the GPC studies, respectively. The Natural Sciences and Engineering Research Council of Canada, le fond FCAR of Quebec, and the University of Montreal are gratefully acknowledged for financial support.

Supporting Information Available: Complete details on the X-ray analysis of **2**, including tables of crystal data, collection and refinement parameters, bond distances and angles, anisotropic thermal parameters, and hydrogen atom coordinates, VT NMR spectra of **3**, and detailed calculations of the equilibrium constant for the reaction of **2** with pyridine, 2-picoline, 3-picoline, 4-picoline, 3,5-lutidine, and PPh₃. This material is available free of charge via the Internet at <http://pubs.acs.org>.

OM010200Z